

The First FIRST Gravitationally Lensed Quasar: FBQ 0951+2635¹

Paul L. Schechter², Michael D. Gregg³, Robert H. Becker^{3,4}, David J. Helfand⁵ and
Richard L. White⁶

ABSTRACT

The $V = 16.9$ quasar FBQ 0951+2635 at redshift $z = 1.24$ appears double on CCD exposures taken in subarcsecond seeing. The two objects are separated by $1''.1$ and differ in brightness by 0.9 mag. VLA observations show the radio source to be double with the same separation and position angle. Spectra taken with the Keck II telescope show the two components to have nearly identical emission line spectra, but with somewhat different absorption line systems. Subtraction of two stellar point spread functions from the pair of components consistently leaves a residual object. Depending upon whether this third object is extended or a point source it may be as much as 1/10 or as little as 1/100 as bright as the brighter QSO component. The observations leave no doubt that the 2 brighter objects are gravitationally lensed images of the same quasar. The third object might be either the lensing galaxy or a third image of the quasar, but both interpretations have serious shortcomings.

Subject headings: cosmology: gravitational lensing — quasars, photometry, spectroscopy

¹Observations reported in this paper were obtained in part at the MDM Observatory, a facility no longer jointly operated by the University of Michigan, Dartmouth College and the Massachusetts Institute of Technology

²Department of Physics, Massachusetts Institute of Technology, Cambridge MA 02139

³Institute of Geophysics and Planetary Physics, Lawrence Livermore National Laboratory, Livermore, CA 94450

⁴Department of Physics, University of California, Davis, CA 95616

⁵Department of Astronomy, Columbia University, 538 West 120th Street, New York, NY 10027

⁶Space Telescope Science Institute, 3700 San Martin Drive, Baltimore MD 21218

1. INTRODUCTION

Quasars that are multiply imaged by gravitational lenses can be used for a wide range of astrophysical investigations (e.g., Kochanek and Hewitt 1996), but the number of known systems is as yet so small that their potential has only begun to be realized. We report here the discovery of a new gravitationally lensed object, FBQ 0951+2635, a $V = 16.9$, 1.7 mJy, $z = 1.24$ quasar drawn from the FIRST Bright QSO Survey (henceforth FBQS; Gregg *et al.* 1996). It has two components with a separation of $1''.1$ and a radio flux ratio of 4:1.

The FBQS offers two advantages as a source of potential gravitational lenses. First, since the quasars are bright, with $R < 17.5$, they are more likely to be lensed than quasars from fainter surveys (Turner *et al.* 1984). Second, since the FBQS quasars are identified using the FIRST radio survey (Becker, White and Helfand 1995; henceforth BWH), radio observations can be used both to confirm the source as a lensed object and to constrain models of the lens.

With these strengths in mind, we undertook to obtain high resolution optical images of quasars identified in the FBQS with the Hiltner 2.4-m telescope at Michigan-Dartmouth-MIT (MDM) Observatory. A short red exposure of FBQ 0951+2635 taken in good seeing immediately revealed two stellar objects, with a separation of roughly $1''$ and a flux ratio of roughly one magnitude. Followup images obtained in V and I showed that the two objects were approximately the same color. Re-examination of the Lick spectrum used to obtain the FBQS redshift showed no sign of stellar features.

Early attempts to obtain spectra of the fainter object were frustrated by poor weather and poor seeing. But an A-array map obtained with the NRAO⁷ Very Large Array (VLA) showed that the radio source was also double, with the same separation and position angle, and roughly the same flux ratio. Radio emission from the fainter component makes it very unlikely that the object is a star – fewer than 0.03% of FIRST radio sources have Galactic stellar counterparts (Helfand *et al.* 1997). Spectra of the two components obtained subsequently with the Keck II telescope are very similar, but not identical.

Longer B, V, R and I exposures obtained in somewhat better seeing during a subsequent MDM run in 1997 January showed evidence for another object not quite colinear with the two quasar components. Though one is tempted to identify this object with the lensing galaxy, the relatively low resolution of the present direct images leaves its character in doubt.

⁷The National Radio Astronomy Observatory is operated by Associated Universities Inc. under a cooperative agreement with the National Science Foundation.

In the sections that follow we describe in greater detail the observations, reductions and arguments which lead us to conclude that FBQ 0951+2635 is gravitationally lensed. We also examine briefly the consequences of two alternative hypotheses regarding the nature of the third object: that it is the lensing galaxy and that it is a third image of the quasar. Both hypotheses present serious difficulties.

2. OBSERVATIONS AND REDUCTIONS

2.1. Initial Optical Imaging

FBQ 0951+2635 is identified as a $z = 1.24$, $B \sim 16.9$ quasar in a forthcoming paper (Becker *et al.* 1997) presenting the second list of FIRST quasars. A spectrum taken at Lick Observatory shows broad lines of Mg II, C III and C IV. The flux at 20 cm is ~ 2 mJy.

A 180 s R filter exposure taken with the Hiltner 2.4 m telescope at MDM Observatory on 1996 December 10 in $0''.9$ seeing showed a double object (cf. Figure 1a), with the fainter component at PA 125° . A 180 s V filter exposure and three 180 s I filter exposures, all with $1''.0$ seeing, were obtained on the same night. Following bias subtraction and flatfielding, an empirical point spread function (PSF) was fit simultaneously to the two objects using a variant of the program DoPHOT (Schechter *et al.* 1993) designed to deal with close point-like and extended objects (Schechter and Moore 1993). The magnitude differences between the brighter and fainter components (henceforth components “A” and “B”) in V , R and I were 0.97, 0.95 and 0.90 mag, respectively, and the separations were $1''.09$, $1''.08$ and $1''.07$ respectively. Both trends are in the sense expected if the lensing galaxy, which should be closer to the fainter component, contaminates it more than the brighter component. The following night, 1996 December 11, was photometric. Images in B , V , R and I were obtained, and reduced as described in §2.4 below.

2.2. Followup Radio Mapping

The system was observed at 3.6 cm with the VLA in the A configuration for 20 minutes on 1996 December 31. The data show clear evidence for duplicity at the same position angle as the optical data (Figure 2). This effectively rules out the possibility that the second optical object is a star randomly projected close to the quasar. Positions and fluxes obtained from this observation are given in Table 1. The larger separation in the radio than in the optical ($1''.12$ as opposed to $1''.08$), if significant, can be understood on the hypothesis that the fainter component is blended with the lensing galaxy.

2.3. Followup Optical Imaging

Additional optical observations were obtained on 1997 January 10 and 11, consisting of 600s exposures in each of B , V , R and I , with an additional 2×500 s obtained in I . The seeing on these images ranged from 0.8 to $0''.9$. When reduced as described above, the separation decreased monotonically going from blue to red. There was also a similar pattern of residuals in each of the images (Figure 3), with a single bright spot slightly east of the A component and north of the B component, and fainter bright rims southwest of each component. The amplitude of the positive residuals is quite small, of order 1-2% of the central intensity of component A. The negative “divots” at the centers of the two components are 3-4% of the central intensity.

The most straightforward interpretation of this pattern of residuals is that there is a third object, roughly midway between the A and B components, slightly to the NE. The two-star model accommodates this third object by bringing the two components closer, giving them a larger flux (and hence leaving large divots) and displacing the two components toward the third object, leaving crescent-like residuals on the opposite side. This pattern is most obvious on the R and I images, less so on the V image and yet less so on the B image, which might be expected if the third object were the lensing galaxy.

An alternate interpretation is that one is simply seeing the consequences of an imperfect template, due to variations in the PSF across the CCD. There are several reasons to think this is not the case. In producing Figure 3, we were careful to use a PSF template which lay within 100 pixels of the quasar. Were the residuals the result of template mismatch, one would see the same pattern associated with both A and B, which seems not to be the case. Moreover the residuals of nearby stars do not show the same pattern. Using other stars as templates show similar patterns, especially on the R and I images.

We therefore undertook to obtain a fit for two point sources plus an extended object (henceforth “C”), which, for the sake of argument we take to be the lensing galaxy, again following the approach of Schechter and Moore (1993). The “galaxy” profile is taken to be a circularly symmetric pseudogaussian, and the positions of both quasar components were treated as free parameters.

The scatter in the galaxy position in these four fits was $0''.04$ in the North-South direction and $0''.10$ in the East-West direction, in both cases small compared to the separation of the two components. The scatters in R.A. and declination for the positions of component B were 15 and 12 mas respectively. The ratio of the flux in the galaxy to that in the brighter component A was roughly 10% in all filters.

The average σ of the pseudogaussian, after correction for seeing, was $0''.510$, which

corresponds to a FWHM somewhat larger than the seeing disk. The average separation between components A and B is $1''.101$, some 20 mas closer than the radio separation. This may be an underestimate, since the redder filters give smaller separations than the bluer, even after allowing for the presence of the lensing galaxy. However the radio separation and position angle applied to the optical image give residuals typical of having enforced too large a separation.

While the trend of smaller separation with redder color appears to be significant, we have adopted, for the present, a straight average of the positions in the four filters as our best guesses of the actual positions, and report these in Table 2. For the purpose of computing commensurable magnitudes, we fix the relative separations at these values. We likewise fix the width of the “galaxy”, object C, at the mean position and shape obtained from the 4 filters. We then fit the data solving only for the overall position of the system and the relative fluxes of the three components, the results of which are also given in Table 2.

It is useful to compare the residuals for the two cases – without the galaxy and with the galaxy and quasar components at their mean positions. These are shown for the R image in Figure 1, along with a low contrast image which shows the component positions. Also shown is the image with A and B subtracted but with the galaxy unsubtracted.

Table 2 shows that the flux ratio of C to A depends surprisingly little on filter, and if anything, gets bluer in the bluest filter. One would expect the lensing galaxy to be considerably redder than the quasar. This leads one to suspect that one is seeing quasar light and not light from the lensing galaxy. This could be either the result of a poor PSF or of a third image of the quasar. We have already argued that the third object is not an artifact of poor PSF fitting. When we try a fit treating the system as three point sources, we find that the fluxes attributed to the third object are very much smaller than when it was treated as a galaxy, and that the colors are no longer so very blue. Our tentative conclusions are first, that the galaxy hypothesis is somewhat more likely, and second, that we are pressing our data to the limits of what it can tell us.

2.4. Photometric and Astrometric Reduction

The data taken on 1996 December 11 included exposures of FBQ 0951+2635 in somewhat poorer seeing and of Landolt (1992) standards in the fields of PG 0231+051 and Rubin 152. The standard and quasar exposures were reduced using routine IRAF reduction programs. We have solved for zeropoint and color terms using “typical” KPNO extinction

coefficients (Massey et al. 1997). Since the standards and the quasar were observed at nearly the same low airmass, the use of typical coefficients (which we take to be uncertain by 30%) introduces errors of at most 0.02 mag for the bright stars in the quasar fields. Photometry for the brightest stars in the quasar field is given in Table 2.

Positions were measured for the brighter stars in the quasar field using the 600s R exposure from January 10, with an empirical PSF used for fitting. This yielded an astrometric solution (relative to the APM astrometry of McMahon and Irwin 1992) with a fractional uncertainty in the scale of 1/750 and with a comparable uncertainty in the rotation of the detector. Positions for these stars, here relative to the quasar A component, are also presented in Table 2. The zeropoint of our astrometric solution differed from the VLA position in Table 2 by almost 1", considerably more than is typical for APM-VLA comparisons. The APM catalog position for the composite A+B shows the same difference.

The empirical PSF fitting described in the previous subsection gives magnitudes for all pointlike objects relative to a template star. With the magnitudes for the template stars now measured, these can now be put on the standard system (after correction for color terms). The results for the quasar are given in Table 2. With a little calculation the pseudogaussian used to model the lensing galaxy can be integrated and a total flux derived. When compared to the reference stars in the field this gives the magnitudes listed in Table 2. It should be noted that our use of a fitting function which falls off more rapidly than a galaxy profile is almost certain to underestimate the brightness of the lensing galaxy.

2.5. Spectroscopy

Spectra were obtained with the Low Resolution Imaging Spectrograph (LRIS) on the Keck II telescope on Valentine's Day 1997. The exposure was 300 seconds in 0".6 seeing. The dispersion of 2".44 Å/pixel gave a resolution of 11 Å. The slit was aligned with the two bright components. Components A and B are clearly resolved spatially along the slit (Figure 4), for which the image scale is 0".215/pixel. The two components (Figure 4) are quite similar, both showing Mg II absorption systems at $z=0.73$ and $z=0.89$. But the emission lines appear to be weaker in the B component than in the A component. The continuum of the B component appears to drop faster than that of the A component beyond 7000 Å, but this may be the result of having intentionally removed the order separating filter. Differences in the equivalent widths of emission lines have been seen in other gravitationally lensed systems (e.g., Wisotzki *et al.* 1993) where it is taken as a sign that the continuum is subject to microlensing.

3. MODELS AND INTERPRETATION

3.1. The Lensing Galaxy Hypothesis

3.1.1. Models for the Lens Potential

Taking the third object to be the lensing galaxy, we have tried fitting several alternative models to the observed positions of components A and B relative to C. Our simplest model, which has the basic features of an elliptical galaxy or dark matter halo, is the singular isothermal quadrupole potential (henceforth SIQP; Kochanek 1991). It produces a flat rotation curve and has equipotentials which are self-similar and roughly, though not exactly, elliptical, and corresponds to a density distribution which is likewise self-similar but not exactly elliptical.

The model has five parameters: a lens strength, b which is roughly half the separation of the images, a shear coefficient γ (which for modest quadrupoles is a factor of 6 smaller than the ellipticity of the underlying mass distribution), an orientation for the shear, and the two angular coordinates of the source with respect to the optical axis defined by the observer and the lensing galaxy. With two pair of coordinates for the quasar images measured with respect to the lensing galaxy, we need one additional constraint. We use the flux ratio of component B to component A. Mao and Schneider (1997) have noted that flux ratios are susceptible to micro- and milli-lensing and are therefore less reliable constraints than the positions.

When we fit this simple model to our observations, we find that the ellipticity of the density is only 0.05, very much rounder than most elliptical galaxies. Alternatively, if one takes the shear to be tidal in origin (and shear is clearly needed because the galaxy is not colinear with the two quasar images and because the flux ratio is very different from unity) one finds a dimensionless shear of only 0.016.

In either case, the quadrupole term is smaller than has been measured in any lens system. A neighboring galaxy with the same potential as the lensing galaxy would have to be at a distance more than 15 times the separation of the two components for its tidal shear to be as small as 0.016. Yet there is another object, probably a neighboring galaxy, some 2" east and slightly south of component B in Figures 1b and 1c. It is also visible in the V and I images (Figure 3).

The near equidistance of object C from components A and B also implies that A and B are both very close to the Einstein ring, and therefore are very highly magnified, with component A magnified by a factor of 30. But the probability of a given magnification varies

roughly inversely as the magnification. The low shear and high magnification indicated by the positions and flux ratio seem very unlikely.

The redder images place the lensing galaxy closer to the fainter component, as is expected. Using only the I filter image gives a larger shear, $\gamma = 0.11$, and more modest magnifications, 5.9 and 2.5. But one is hard pressed to explain why the bluer images give a third object closer to A component. If there were a central component, C', contaminating what we have taken to be the galaxy, one would expect it to be on the same side of the lensing galaxy as the intermediate distance component. Component C' should be between the galaxy and B rather than on the other side.

3.1.2. The SED of the Lensing Galaxy

For the purpose of predicting the apparent magnitude of the lensing galaxy, we assume that the lensing potential is a that of a singular isothermal sphere with associated line of sight velocity dispersion σ . If the potential has strength b , the associated velocity dispersion is given by

$$\frac{\sigma^2}{c^2} = \frac{D_S}{D_{LS}} \frac{b}{4\pi} \quad , \quad (1)$$

where D_S and D_{LS} are, respectively, angular diameter distances to the source and from the lens to the source (Narayan and Bartelmann 1997), with b measured in radians. For FBQ 0951+2635 $b \sim 0''.55$. Following Keeton *et al.* (1997) we take

$$\frac{L}{L^*} = \left(\frac{\sigma}{220 \text{ km/sec}} \right)^4 \quad \text{and} \quad (2)$$

$$\frac{L}{L^*} = \left(\frac{\sigma}{144 \text{ km/sec}} \right)^{2.6} \quad (3)$$

for early and late type galaxies, respectively, where L^* corresponds to $M_B^* = 19.7 + 5 \log h$. For any assumed redshift we can calculate a predicted velocity dispersion and distance modulus,

$$m_{AB}(\lambda_{obs}) - M_{AB}(\lambda_{rest}) = 5 \log(D_L) + 7.5 \log(1 + z) \quad , \quad (4)$$

where D_L is again an angular diameter distance. Here m_{AB} , the predicted apparent magnitude, depends both on the measured separation and the assumed redshift. Adopting standard absolute spectral energy distributions (SEDs) for a giant elliptical galaxy and an Scd spiral from the HST WFPC2 handbook (Burrows *et al.* 1995) and normalizing these at $4000(1 + z) \text{ \AA}$ gives us predicted SEDs. As redshift increases the curves move to redder wavelengths and fainter apparent magnitudes while preserving the shapes of the SEDs.

The photometry of Table 2 can be transformed to the m_{AB} system by adding -0.17, 0.00, 0.18 and 0.33 mag, respectively, to the observed B , V , R and I apparent magnitudes. For the sake of comparison we have computed the predicted SEDs for a giant elliptical at redshift of 0.2 and an Scd spiral at a redshift of 0.4. These predict a V magnitude close to the observed value, but it is clear from Figure 5, first, that the observed colors are too blue and second, that only a very late type galaxy at very low redshift could produce colors as blue as those observed. Such a galaxy would be far brighter than the third object.

3.2. The Third-Image Hypothesis

As is evident from the above discussion, models interpreting the third object as the lensing galaxy have serious deficiencies. Since it is substantially fainter than the other two, one might suppose the third object to be a demagnified image associated with the core of the lensing galaxy. But unless the core radius were very large, such an image would lie very close to the center of the galaxy, again giving an implausibly small impact parameter and the corresponding large magnifications. Models of this sort have three additional free parameters beyond those described in the previous section, a core radius and the two coordinates of the lensing galaxy (now taken to be unknown) giving a total of eight free parameters. The 6 coordinates for the three components and the two magnification ratios give eight constraints. In our (admittedly limited) experimentation with such models we found the solutions to be quite unstable.

A more exotic variant of the third-image hypothesis is that we are seeing a three-image configuration associated with a galactic disk (Keeton and Kochanek 1997). The disk (like a uniform edge-on sheet) produces two images which straddle it. If the disk is not quite edge-on, and has a finite projected density at its midplane, a third image will form close to the midplane, in the same way that a third image forms inside the core radius of a non-singular isothermal sphere. In the present case the non-collinearity of the three components would then call for a degree of central concentration deflecting the midplane image more than the two straddling images. Again the added degrees of freedom make fitting such models a frustrating exercise.

But just as the colors are troublesome when we force object C to have the same extended shape in all filters, the colors are troublesome when we assume that object C is a point source. As described in §2.3, when we treat the system as three point sources we find that component C is much redder than the other two. This might still be consistent with the third-image hypothesis, but only if the third component were reddened by dust in the lensing galaxy.

3.3. A Working Hypothesis: Blame the Data

The difficulties with both hypotheses regarding the third object are traceable to the B filter image. The B filter position of the third image forces very round potentials and large magnifications. The B filter apparent magnitude is likewise the most inconsistent with either hypothesis. Since we have only one B exposure in good seeing, one might imagine some unmodeled phenomenon is affecting the data – a cosmic ray or a non-linear pixel response – or simply an error in the data reduction. In many ways this is more palatable than either physical model for the observations. Still another alternative is that the system is yet more complicated with perhaps both a third quasar component and a lensing galaxy of comparable brightness.

4. SUMMARY AND CONCLUSIONS

We have discovered a new gravitationally lensed quasar, with two components which are confirmed images of the quasar and a third object which might either be the lensing galaxy or another quasar image. Both hypotheses for the third object have serious shortcomings. Possible explanations for these difficulties include corrupt data, an error in the data reduction and analysis, or a yet more complicated geometry on scales too small to be resolved with the present observations.

We gratefully acknowledge support for the FIRST survey from NRAO, the National Science Foundation (grants AST94-19906 and AST94-21178), the IGPP/LLNL (DOE contract W-7405-ENG-48), the STScI, the National Geographic Society (grant NGS 5393-094), NATO (grant CRG 950765), Sun Microsystems, and Columbia University. PLS gratefully acknowledges financial support from NSF grant AST96-16866.

REFERENCES

- Becker, R. H., White, R. L., Helfand, D. L. 1995, *ApJ*, 450, 559
- Becker, R. H., et al., 1997, in preparation
- Burrows, C. J., et al., 1995, in C. J. Burrows, ed., *Wide Field and Planetary Camera 2 Instrument Handbook*, (Baltimore: STScI), version 3.0, p. 67
- Gregg, M. D., Becker, R. H., White, R. L., Helfand, D. J., McMahon, R. G., and Hook, I. M. 1996, *AJ*, 112, 407
- Helfand, D. J., Schnee, S. Becker, R. H., White, R. L. and McMahon, R. G. 1997, in preparation
- Keeton, C. R., and Kochanek, C. S., 1997, preprint astro-ph/9705093
- Keeton, R. R., Kochanek, C. S., and Falco, E. E. 1997, preprint astro-ph/9708161
- Kochanek, C. 1991, *ApJ*, 373, 354
- Kochanek, C. S., and Hewitt, J. N. 1996, *IAU Symposium 173: Astrophysical Applications of Gravitational Lensing*, Dordrecht: Kluwer
- Landolt, A. U. 1992, *AJ*, 104, 340
- Massey, P., Armandroff, T., De Veny, J., Claver, C., Harmer, C., Jacoby, G., Schoening, B., and Silva, D. 1997, *Direct Imaging Manual for Kitt Peak*, Tucson: NOAO, p. 29
- McMahon, R. G., and Irwin, M. J. 1992, in *Digitized Optical Sky Surveys*, eds. H. T. McGillivray and E. B. Thomson, Dordrecht: Kluwer, p. 417
- Mao, S. and Schneider, P. 1997, preprint, astro-ph/9707187
- Narayan, R. and Bartelmann, M., 1996, *Formation and Structure of the Universe*, A. Dekel and J. Ostriker, Cambridge: Cambridge University Press.
- Schechter, P. L. and Moore, C. B., 1993, *AJ*, 105, 1
- Schechter, P. L., Mateo, M., and Saha, A., 1993, *PASP*, 105, 1342
- Turner, E. L., Ostriker, J. P., and Gott, J. R. III 1984, *ApJ*, 284, 1
- Wisotzki, L., Köhler, T., Kayser, R., and Reimers, D. 1993, *A&A*, 278, L15

Fig. 1.— a) A 600 s R filter direct image of FBQ 0951+2635 at low contrast. The brighter component, A, is N (up) and W (to the right) of B. b) The same image (at higher contrast) after simultaneous fitting of a stellar PSF to A and B and subtracting. c) The same image after simultaneous fitting of two stellar PSFs and a pseudogaussian and subtracting. d) The same image with stellar PSFs subtracted but without subtracting the pseudogaussian. Panels b), c) and d) are at factors of 50, 50, and 17 higher contrast, respectively, than panel a).

Fig. 2.— VLA A-array map of FBQ 0951+2635 with contours plotted at 3, 6, 12, 24 and 50 times the RMS noise.

Fig. 3.— B , V , R , and I images of FBQ 0951+2635. North is up and East is to the left. For each filter empirical stellar PSFs have been fitted to the A and B components and subtracted from the image. The pattern of residuals suggests a third object to the NE of of A and B.

Fig. 4.— Upper panel: Spectra of the A and B components of FBQ 0951+2635. Lower panel: the ratio of the A and B components, after normalizing at 5000 Å. Inset: a cut perpendicular to the spectrum, showing the 5 pixel separation between the A and B components.

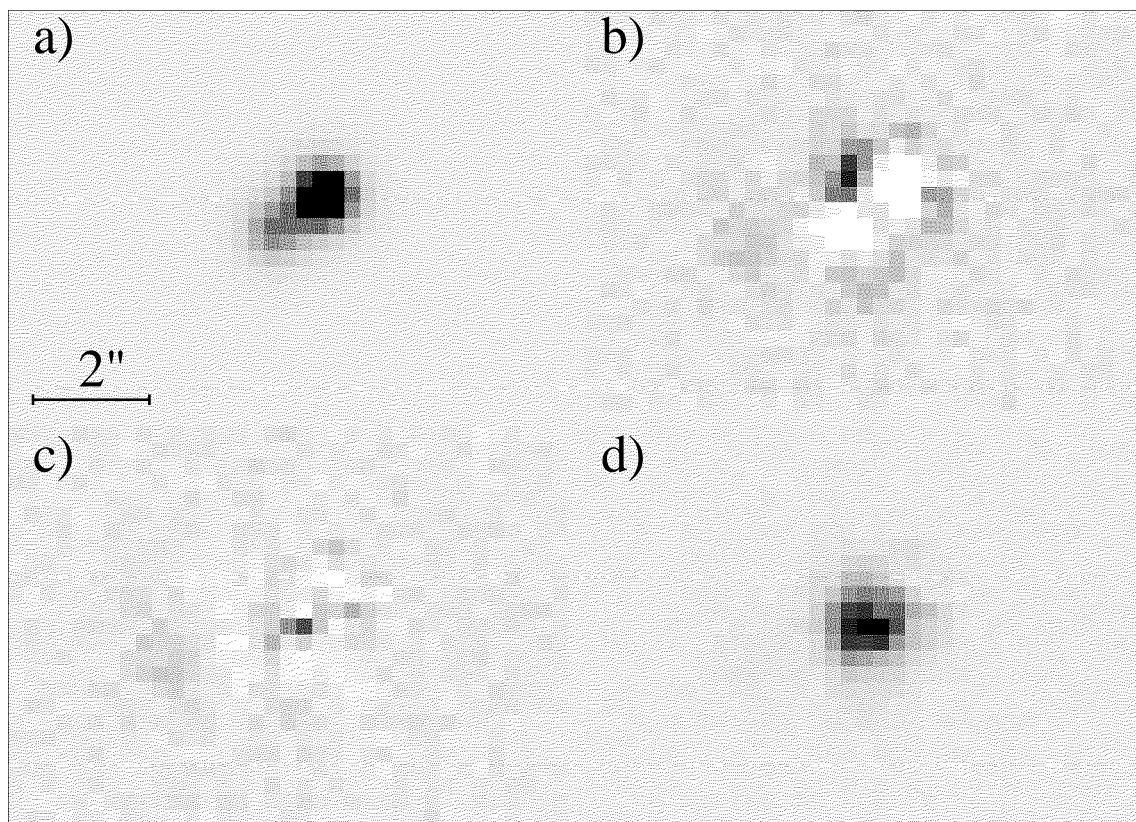
Fig. 5.— Predicted AB apparent magnitude as a function of wavelength for the lensing galaxy assuming either the SED typical of a giant elliptical (solid line) galaxy or that of a late type Scd galaxy (dashed line). The points are AB magnitudes for the lensing galaxy corresponding (left to right) to the B , V , R , and I photometry of Table 2. Redshifts for the SEDs were chosen to agree with the observed image separation and V filter photometry.

Table 1. FBQ 0951+2635: VLA A Array Observations

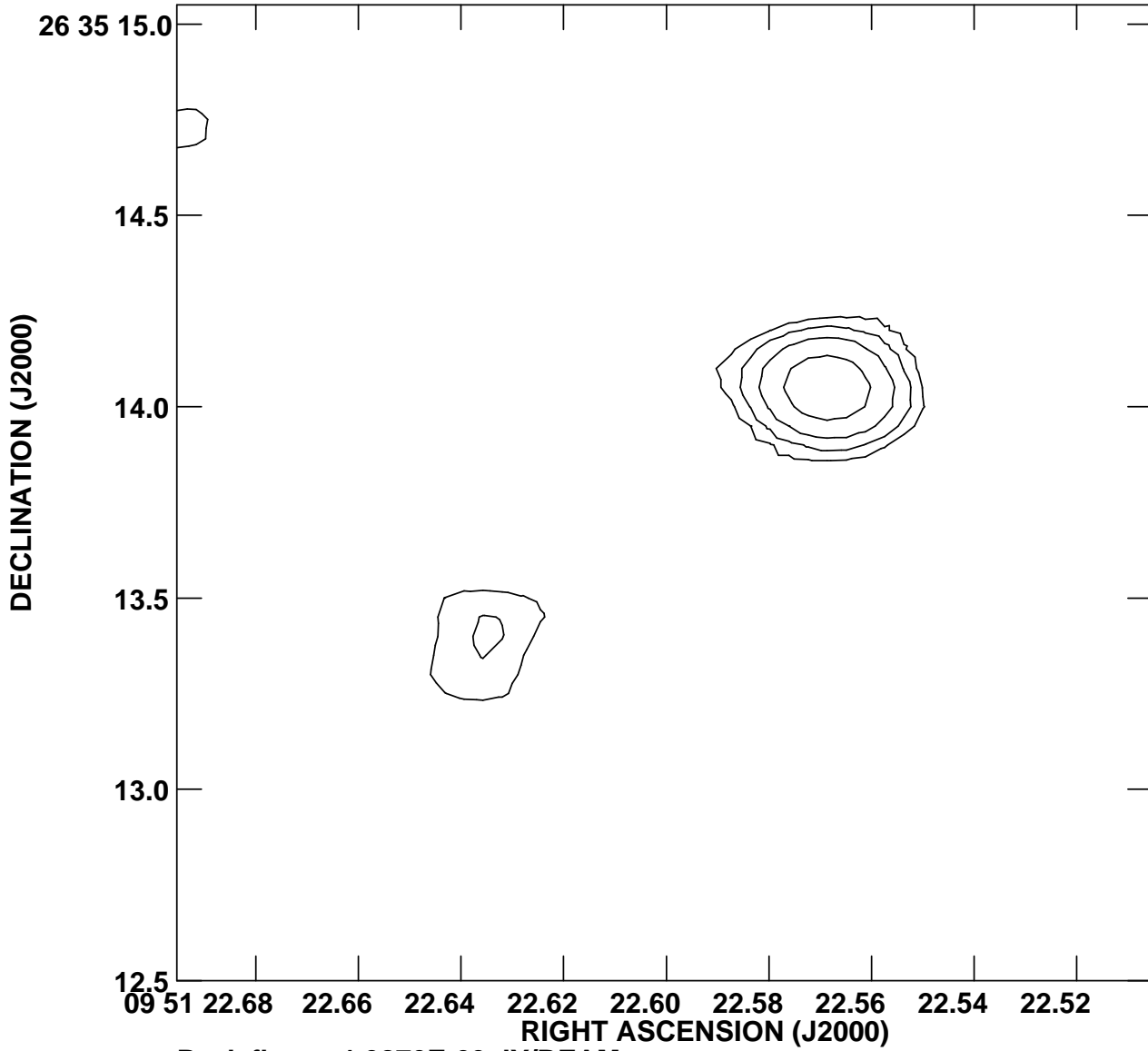
Obj.	RA(2000)	Dec(2000)	$f_{8.4GHz}$
A	09 51 22.569	+26 35 14.05	1.4 mJy
B	09 51 22.636	+26 35 13.38	0.3 mJy

Table 2. Astrometry and photometry for FBQ 0951+2635 and nearby stars

Obj.	Δ RA (s)	Δ Dec (")	V	B-V	V-R	R-I
A	0.	0.	17.31	0.35	0.29	0.28
B	+0.0669	-0.638	18.25	0.30	0.27	0.29
C	+0.0413	-0.220	20.00	0.25	0.40	0.36
05	+5.678	-116.27	16.484	1.397	0.878	0.931
22	-1.197	-36.98	17.454	1.332	0.842	0.862
28	-6.810	-18.98	17.119	0.901	0.528	0.513
30	-7.472	+50.88	16.206	0.778	0.451	0.439
34	-8.321	+32.37	18.027	1.602	1.082	1.397



PLot file version 2 created 06-AUG-1997 17:16:42
G0951+26 IPOL 8460.100 MHZ G0951+2635.ICLN.6



Peak flux = 1.3870E-03 JY/BEAM
Levs = 3.5000E-05 * (3.000, 6.000, 12.00,
24.00, 50.00, 100.0, 200.0)

